Fluid–fluid and fluid–solid phase separation in nonadditive asymmetric binary hard-sphere mixtures

2005 J. Phys.: Condens. Matter 17 771

(http://iopscience.iop.org/0953-8984/17/6/001)

INSTITUTE OF PHYSICS PUBLISHING JOURNAL OF PHYSICS: CONDENSED MATTER

J. Phys.: Condens. Matter **17** (2005) 771–796 doi:10.1088/0953-8984/17/6/001

Fluid–fluid and fluid–solid phase separation in nonadditive asymmetric binary hard-sphere mixtures

F Lo Verso[1], **D Pini and L Reatto**

Istituto Nazionale di Fisica della Materia and Dipartimento di Fisica, Università di Milano, Via Celoria 16, Milano, Italy

E-mail: federica.loverso@mi.infn.it

Received 11 October 2004, in final form 23 December 2004
Published 28 January 2005
Online at stacks.iop.org/JPhysCM/17/771

Abstract

Very asymmetric mixtures of hard spheres naturally arise in the modellization of colloidal dispersions. Effective potentials have emerged as a powerful tool for describing these systems and have often been employed to extract the phase diagram in both the additive and nonadditive cases. However, most theoretical investigations have been carried out by means of mean-field-like approaches, so their quantitative accuracy remains to be assessed. Here we employ previously determined effective potentials for nonadditive hard-sphere mixtures to study the fluid–fluid phase transition by the hierarchical reference theory (HRT), which is designed to take realistically into account the effects of long-range fluctuations on phase separation. Fluid–solid equilibrium is addressed by supplementing HRT with thermodynamic perturbation theory for the solid phase. We apply this approach both to a potential with adjustable nonadditivity parameter (Louis *et al* 2000 *Phys. Rev.* E **61** R1028) and to the Asakura–Oosawa (AO) potential, which represents an extreme case of nonadditivity. Our results for the phase diagram, including modified hypernetted chain (MHNC) calculations, are compared to those of other liquid-state theories and are found to agree nicely with available simulation data. Unlike commonly adopted liquid-state theories, HRT is capable both of getting arbitrarily close to the fluid–fluid critical point, and of giving nontrivial critical exponents. In particular, the fluid–fluid coexistence curve is much flatter than that obtained via perturbation theory, in agreement with a recent finite-size scaling Monte Carlo analysis of the AO model.

[1] Present address: Institut für Theoretische Physik II, Heinrich-Heine-Universität Düsseldorf, Universitätsstrasse 1, Düsseldorf, Germany.

0953-8984/05/060771+26$30.00

1. Introduction

During the past years the hard-sphere (HS) system has been studied in detail: this simple model is ideally suited for the study of phenomena in which the hard core of the potential is the dominant factor and it represents a standard reference system for determining the properties of realistic models. Now its phase diagram is well understood: a pure hard-sphere fluid does not undergo a liquid–gas transition, but shows a well defined freezing transition driven by purely entropic effects [1, 2]. Binary hard-sphere mixtures represent a very important system either for a similar reference role for binary mixtures of simple fluids or as a model for mixtures of colloids and polymers and other colloidal systems (see for example [3]).

One of the most studied models is that of additive HS where the cross diameter is $\sigma_{12} = (\sigma_1 + \sigma_2)/2$, σ_1 and σ_2 being the diameters of the two species of particles. Such a mixture of large and small particles exhibits an interesting competition between demixing into dilute and concentrated suspensions of large particles, driven by the osmotic depletion effect [4], and freezing into an ordered crystalline phase. Monte Carlo simulations [5] of binary additive hard-sphere mixtures with size ratio $q = \sigma_2/\sigma_1 \leqslant 0.2$ have shown that the demixing transition is pre-empted by freezing of a low-concentration disordered 'fluid' phase into an fcc crystal of large particles. In that paper the authors also determine an effective one-component description: the derivation of an effective potential is in principle a powerful tool for studying the behaviour of an asymmetric binary mixture, at least for size-ratios $q \leqslant 0.3$. For such a size ratio many-body interactions are not very important [6], while at the same time a direct confirmation of the fluid–fluid demixing transition by computer simulations is difficult because of slow equilibration problems.

On the other hand, experiments on sterically or charge-stabilized binary 'hard-sphere' colloids are shown to exhibit nonadditive behaviour, i.e. $\sigma_{12} = (\sigma_1 + \sigma_2)(1 + \Delta)/2$ where the parameter of nonadditivity Δ can be positive or negative (see e.g. [7, 8]). An extreme case of nonadditivity was studied by Widom and Rowlinson, who considered $\sigma_1 = \sigma_2 = 0$ and $\sigma_{12} > 0$ [9]. For this system they showed the presence of a demixing transition. Another example is the simplest Asakura–Oosawa (AO) model of colloid–polymer mixtures, described in section 4. This model describes a binary mixture of polymers and colloids: the polymers are assumed to be noninteracting; however, they are excluded from the colloids to a certain centre-of-mass distance. Louis *et al* [7] propose that the effect of a wide variety of extra interactions on depletion potentials can be understood by a simple mapping onto a nonadditive HS mixture model. In [10] the authors show that the formal procedure of integrating out the degrees of freedom of the small spheres in a binary hard-sphere mixture works equally well for nonadditive as it does for additive mixtures. Using a density-functional treatment originally developed for additive hard-sphere mixtures they obtain the zero-, one-, and two-body contributions of the effective Hamiltonian. Even a small degree of positive nonadditivity of the diameter σ_{12} has significant effects on the shape of the depletion potential and on the phase behaviour, as it might drive the demixing transition from metastable to stable. Moreover, Vliegenthart and Lekkerkerker [11] have shown that the fluid–fluid critical point of many one-component fluids occurs when the reduced second virial coefficient is approximately equal to 1.5. This works well for the depletion potential simulations of Dijkstra *et al* [5, 12, 13], suggesting that this accurate criterion can also be used to predict the effect of nonadditivity on fluid–fluid phase separation [7].

Although the qualitative phase behaviour of highly asymmetric binary mixtures as a function of q and Δ is known (see e.g. [4, 7, 10, 14]), theoretical studies of these systems have been carried out mainly by means of mean-field-like approaches, such as standard thermodynamic perturbation theory. As already pointed out in previous studies [12], this

can entail a considerable degree of quantitative inaccuracy, especially as far as the fluid region of the phase diagram is concerned. The main purpose of this paper is to employ the effective potentials previously obtained by other authors to investigate fluid–fluid phase separation by means of the hierarchical reference theory (HRT) [15]. This renormalization-group based method has already proved quite reliable in describing the phase diagram of simple one- and two-component fluids interacting via Lennard-Jones-like potentials as well as Coulombic fluids and spin systems, so it is indeed tempting to test its accuracy for a different kind of interactions such as the effective potentials considered here. HRT is designed to take realistically into account the effects of long-range fluctuations on phase separation, giving more accurate results than commonly adopted liquid-state theories. We also address the fluid–solid transition by supplementing HRT with thermodynamic perturbation theory for the solid phase: the rationale for doing so is that, as pointed out before [12], thermodynamic perturbation theory is expected to be much more accurate for the solid than for the fluid. Moreover, long-wavelength fluctuations play a minor role in a strongly first-order transition like the fluid–solid one.

We first investigated a nonadditive, asymmetric HS mixture for very different size ratios and different values of the nonadditivity parameter as modelled by the pair interaction obtained in [4]. We then turned to an extreme instance of a nonadditive HS mixture, namely the AO model. Our results for the phase diagram were compared with those obtained from thermodynamic perturbation theory [4, 12] and MC simulations [12].

The overall qualitative picture that emerges from the present study agrees with that expected on the basis of previous investigations: specifically, positive nonadditivity is predicted to stabilize the depletion-induced fluid–fluid demixing transition with respect to freezing, while decreasing the size ratio q has the opposite effect. However, significant quantitative differences appear: for instance, in the AO case, if thermodynamic perturbation theory is used also for the fluid phases, the crossover from stable to metastable fluid–fluid phase separation is located at $q \lesssim 0.31$ [12], while the HRT prediction is $q \lesssim 0.45$, in closer agreement with the MC result $q \lesssim 0.4$ [12]. Moreover, unlike standard liquid-state theories, HRT gives nonclassical critical exponents. As a consequence, the curvature of the fluid–fluid coexistence curve in the neighbourhood of the critical point is accurately reproduced, as shown by the comparison of our results with a recent MC study supplemented by finite-size scaling [16, 17].

We find these results very encouraging, especially in view of the fact that the closure relation that we used in our HRT scheme is tailored to Lennard-Jones-like potentials rather than to the effective potentials describing depletion-induced interactions in colloidal systems. In particular, no special care was adopted to accurately take into account the effect on the correlations of the narrow and deep attractive well which characterizes the latter class of potentials and accounts for the main qualitative differences with respect to atomic and molecular fluids [18]. Nevertheless, the thermodynamics obtained within our approach appears to be quite accurate.

Besides HRT, we also performed few calculations by the modified hypernetted chain (MHNC) integral equation. In a previous study [19] we concluded that the MHNC gives quite a good description of the fluid–fluid coexistence region of highly asymmetric additive hard-sphere mixtures described by an effective pair interaction (see also [20]). However, determining the phase diagram by MHNC is quite cumbersome, so we used this integral equation just to determine the spinodal curves of nonadditive mixtures, in order to locate the critical point and estimate the coexistence region.

This paper is organized as follows: first of all, in section 2 we present the theoretical tools we utilized to study nonadditive hard-sphere mixtures. In section 2.1 we present a brief introduction to the HRT. In section 2.2 we present the perturbation theory that we used

to determine the chemical potential and the pressure of the solid phase. In section 2.3 we introduce the modified hypernetted chain integral equation.

Section 3 deals with a general model for nonadditive, asymmetric HS mixtures. In section 3.1 we introduce the pair potential that we used to model the interaction between large spheres. In sections 3.2 and 3.3 we describe our results for the phase diagram obtained respectively by MHNC and HRT and compare them to those obtained by means of other fluid-state theories and MC simulations.

In section 4 we turn to the AO model. In section 4.1 we recall the AO model and the form of the AO pair interaction. In section 4.2 we assess the accuracy of the HRT to study the phase diagram of the AO model, comparing our results with MC simulations and perturbation theory results. In section 4.3 we discuss the effects of critical fluctuations on the demixing transition, specifically on the coexistence curve, the reduced compressibility, and the correlation length. Finally in section 5 we summarize our study and draw our conclusions.

2. Theory

2.1. Hierarchical reference theory

The HRT approach has already been discussed in detail in previous work [15, 21, 22], so here we give just a brief summary.

We consider a fluid of particles interacting via a spherically symmetric potential $v(r)$. We assume that $v(r)$ can be split into the sum of a singular contribution $v_{\mathrm{R}}(r)$ which accounts for the short-range repulsion between the particles, and a longer-ranged tail $w(r)$ which may induce fluid–fluid phase separation. The properties of the fluid interacting via the repulsive potential $v_{\mathrm{R}}(r)$ alone are considered as known, so that it acts as a 'reference' or unperturbed system. For a hard-core plus tail potential like those considered in this work, the natural choice of the reference system is the hard-sphere fluid. The HRT differs from the conventional liquid-state approaches in the way the attractive perturbation is dealt with. In order to accurately describe the long-range fluctuations that are important in criticality and phase separation, the attractive part of the interaction is switched on gradually by introducing a Q-*system* with a modified interaction $v_Q(r) = v_{\mathrm{R}}(r) + w_Q(r)$, where $w_Q(r)$ is defined in such a way that its Fourier transform $\tilde{w}_Q(k)$ coincides with that of the original attractive potential $\tilde{w}(k)$ for $k > Q$, and vanishes for $k < Q$. The introduction of such an infra-red cut-off in the interaction is physically equivalent to inhibiting fluctuations with characteristic lengths $L > 1/Q$. If Q is made to evolve from $Q = \infty$ down to $Q = 0$, the Q-systems evolve from the reference system by acquiring fluctuations of longer and longer wavelengths. The fully interacting system is recovered as the $Q \to 0$ limit of such a process. Only in this limit are true long-range correlations allowed to develop in the fluid, if it is close to a critical point. The equation for the corresponding evolution of the Helmholtz free energy A_Q of the Q-systems can be determined exactly and is related to the perturbation in momentum space $\Phi(k) = -\beta\tilde{w}(k)$ with $\beta = 1/(k_{\mathrm{B}}T)$, and to the direct correlation function of the Q-system in momentum space $c_Q(k)$. The evolution equation for the Helmholtz free energy is most easily formulated in terms of a modified free energy $\mathcal{A}_Q$ and direct correlation function $\mathcal{C}_Q(k)$ defined as

$$\mathcal{A}_Q = -\frac{\beta A_Q}{V} + \frac{1}{2}\rho^2\left[\Phi(k=0) - \Phi_Q(k=0)\right] - \frac{1}{2}\rho\int\frac{\mathrm{d}^3\mathbf{k}}{(2\pi)^3}\left[\Phi(k) - \Phi_Q(k)\right] \tag{1}$$

$$\mathcal{C}_Q(k) = c_Q(k) + \Phi(k) - \Phi_Q(k), \tag{2}$$

where V is the volume of the system. The HRT equation for $\mathcal{A}_Q$ is then

$$\frac{\partial \mathcal{A}_Q}{\partial Q} = -\frac{Q^2}{4\pi^2} \ln\left(1 - \frac{\Phi(Q)}{\mathcal{C}_Q(Q)}\right). \tag{3}$$

For $Q \to 0$, i.e. at the end of the evolution process, the modified quantities $\mathcal{A}_Q$, $\mathcal{C}_Q$ yield respectively the true free energy and direct correlation function of the fully interacting system. For $Q = \infty$, $\mathcal{A}_Q$ and $\mathcal{C}_Q$ are nothing but the mean-field free energy and the random-phase approximation direct correlation function in the presence of the full perturbing potential $\Phi(k)$. These play the role of the initial conditions of the evolution equation (3), which then describes how the mean-field estimate for the free energy is affected by the inclusion of fluctuations. This equation is manifestly not closed, since the evolution of the free energy $\mathcal{A}_Q$ is related to the direct correlation function $\mathcal{C}_Q(k)$, which is itself unknown. In fact, equation (3) is just the first equation of an infinite hierarchy for the direct correlation functions of increasing order. A point of crucial importance in order to implement a viable HRT scheme is then supplementing equation (3) with a closure relation involving $\mathcal{C}_Q(k)$. Here, as well as in the previous applications of HRT, we have adopted for $\mathcal{C}_Q(k)$ an approximate form inspired by standard perturbative liquid-state theories:

$$\mathcal{C}_Q(k) = c_{\mathrm{HS}}(k) + \lambda_Q \Phi(k) + \mathcal{G}_Q(k). \tag{4}$$

In the above expression, $c_{\mathrm{HS}}(k)$ is the Fourier transform of the direct correlation function of the hard-sphere reference system, which can be accurately represented by the Verlet–Weis parametrization [23], while λ_Q and $\mathcal{G}_Q(k)$ are *a priori* unknown, state-dependent quantities to be determined on the basis of two constraints related respectively to the long- and the short-range behaviour of the correlations. Specifically, the amplitude λ_Q of the perturbation is determined in such a way that each Q-system satisfies the compressibility sum rule which expresses the isothermal compressibility in terms of the zero-wavevector value of the structure factor, or equivalently of the direct correlation function in momentum space:

$$\mathcal{C}_Q(k = 0) = \frac{\partial^2 \mathcal{A}_Q}{\partial \rho^2}, \tag{5}$$

where ρ is the number density of the fluid. The function $\mathcal{G}_Q(k)$ is instead chosen so that the radial distribution function $g_Q(r)$ of each Q-system satisfies the condition $g_Q(r) = 0$ for $0 < r < \sigma$, σ being the hard-sphere diameter. This requirement stems from the singular interparticle repulsion due to the reference part of the interaction. In terms of the direct correlation function $c_Q(k)$ it amounts to

$$\int \frac{\mathrm{d}^3\mathbf{k}}{(2\pi)^3} \exp[\mathrm{i}\mathbf{k}\cdot\mathbf{r}] \left[\frac{1}{\rho c_Q(k)} + 1\right] = \rho \qquad 0 < r < \sigma. \tag{6}$$

Implementing the thermodynamic consistency condition (5) in equation (3) gives a partial differential equation (PDE) for $\mathcal{A}_Q$, which involves both the first partial derivative of $\mathcal{A}_Q$ with respect to Q, and its second partial derivative with respect to the density ρ. This PDE, supplemented by suitable initial (i.e., for $Q = \infty$) and boundary (i.e., for low and high density) conditions, is integrated numerically down to $Q = 0$. The details of the procedure have been given elsewhere [22]. Here we would like to recall the two approximations entailed by the scheme outlined above, since they can be relevant for the applications considered in this work. First, equation (4) assumes that the direct correlation function of the fluid depends linearly on the perturbation $\Phi(k)$. This ansatz is most adequate when the perturbation range is much longer than that of the reference part of the interaction, i.e. of the particle size. For short-range perturbations, nonlinear contributions which are not accounted for by the present closure are expected to become important [24]. A more technical but at least equally relevant point is related to the implementation of the core condition (6). Following a widely adopted

procedure in liquid-state theory, the inverse Fourier transform of the function $\mathcal{G}_Q(k)$ has been expanded in series of Legendre polynomials in the interval $0 < r < \sigma$, and the series has been truncated after a finite number of terms (typically five). The evolution equations for the expansion coefficients were then determined by differentiating the integral equation (6) for $c_Q(k)$ with respect to Q, and subsequently projecting it on the polynomials used in the expansion. However, the resulting equations are coupled to the evolution equation (3) for the free energy, and this makes them difficult to handle. Therefore, as described in detail in [21, 22], in the derivative of $c_Q(k)$ with respect to Q the long-wavelength contributions containing the isothermal compressibility of the Q-system were disregarded. Physically this amounts to decoupling the short- and the long-range evolution of the correlations. Again, this approximation is fully justified for long-range perturbations, where the short- and the long-range part of the correlations are mainly affected by the reference and the perturbation term respectively, but becomes more problematic for short-range interactions where the interplay between excluded-volume and cohesion effects is much stronger. We will return to this point in section 4.

Finally we observe that, in previous applications of HRT, fluid–fluid phase separation was driven by the temperature T via the factor β that determines the strength of the perturbation $\Phi(k)$ in equation (3). Since in the present work the potentials that we will be considering refer to athermal systems one can set $\beta = 1$. In this case phase separation is governed by the density of the small particles responsible for the depletion interaction between larger particles. We remark that state dependent pair potentials arise from coarse-graining procedures in condensed matter physics. In principle, as discussed in detail in [25], the particular coarse-graining procedure utilized to determine the effective pair interaction is important to determine correctly physical properties of interest. The McMillan–Mayer procedure to trace out the smaller component in solution in the framework of the semi-grand ensemble maps the two-component mixture onto a useful effective one-component description (see for example the discussion about the AO model in [25]). In particular, the effective partition function obtained, as long as the fugacity of the small spheres is fixed as an external parameter, can be interpreted as that of an effective one-component system, not state dependent. Then in both cases (temperature and density of the small spheres) the quantity which sets the interaction strength appears in equation (3) as a parameter. This does not imply any substantial change in our treatment.

2.2. Perturbation theory

In order to determine the fluid–solid phase boundary, we need the free energies of both the fluid and solid phases. While the free energy of the fluid has been obtained by HRT, for the free energy of the solid we have resorted to standard thermodynamic perturbation theory. This can be regarded as the application to a solid reference system of the perturbative expansion in powers of the inverse temperature β originally developed for a fluid by Barker and Henderson [26]. The Helmholtz free energy per unit volume A_s/V of a solid interacting via a hard-sphere plus tail potential $v(r) = v_R(r) + w(r)$ then reads

$$\frac{\beta A_s}{V} = \frac{\beta A_s^{HS}}{V} + \frac{1}{2}\beta\rho^2 \int d^3\mathbf{r}\, g_s^{HS}(r)\, w(r) + \frac{\beta A_2}{V} + \mathcal{O}(\beta^3), \tag{7}$$

where A_s^{HS} and g_s^{HS} are the Helmholtz free energy and the radial distribution function of the hard-sphere solid averaged over the solid angle, and $\beta A_2/V$ denotes the second-order term in β. Solid-state perturbation theory has already been adopted many times for studying fluid–solid equilibrium [27] and how this transition is affected by the range of the interaction [12, 28, 29]. Use of the truncated expansion (7) for the solid phase has proved to be quite reliable, actually

considerably more so than in the fluid region [12]. Following previous investigations [12, 28], equation (7) has been truncated at the second-order term, which has then been estimated by an approximation suggested by Barker and Henderson [26], namely

$$\frac{\beta A_2}{V} \simeq -\frac{1}{4}\beta^2\rho^2\chi_s^{HS}\int d^3\mathbf{r}\, g_s^{HS}(r)w^2(r), \tag{8}$$

where χ_s^{HS} is the compressibility of the hard-sphere solid divided by the ideal-gas value. We observe that for the athermal systems considered in this work $\beta w(r)$ does not depend on temperature, so that β does not appear explicitly in the expansion. The Helmholtz free energy of the hard-sphere crystal needed in equation (7) has been determined by integrating with respect to density the equation of state given by Hall [30], which expresses the compressibility factor $Z = \beta P/\rho$ of the hard-sphere solid as an expansion in powers of the relative deviation of the density from its value at close packing $\rho_{cp} = \sqrt{2}\sigma^{-3}$. As in [31], the integration constant is given by the value of A_s^{HS} at a density $\rho = 0.736\,\rho_{cp}$, for which we have used the result, also reported in [31], $\beta A_{ex}^{HS}/N = 5.918\,89$, N being the particle number, determined via numerical simulation by Frenkel for the excess free energy per particle with respect to the ideal gas. The radial distribution function of the hard-sphere solid has been represented by the parametrization of Kincaid and Weis [32]. The potentials considered here are strictly vanishing beyond a certain distance, so the integrals involving $g_s^{HS}(r)$ in equations (7) and (8) are actually restricted to a finite interval. Fluid–solid equilibria were determined by equating the pressure and the chemical potential of the fluid phase determined by HRT with those of the solid phase obtained from equations (7), (8).

2.3. Modified hypernetted chain integral equation

As specified above, we studied the structure and the thermodynamical behaviour of nonadditive mixtures also by means of the modified hypernetted chain integral equation (MHNC). In this way we could test the efficiency of the MHNC closure for describing the properties of deep and narrow potentials, with respect to MC simulation results or other liquid-state theories previously utilized to study this system. In addition, we checked the agreement between MHNC closure and HRT theory.

The MHNC equation is in general accurate for describing the structure and the thermodynamical behaviour of systems described by repulsive interactions as well as when an attractive contribution to the interaction is present [33, 34]. Recently, it has been verified that this theory is also remarkably accurate for ultrasoft-core potentials [35]. This equation starts from an exact relation [36], obtained from a cluster expansion, which connects the radial distribution function (rdf) $g(r)$ to the interparticle potential $v(r)$:

$$g(r) = \exp[-\beta v(r) + h(r) - c(r) + E(r)]. \tag{9}$$

$h(r) = g(r) - 1$ and $c(r)$ are the pair and the direct correlation function, respectively. $c(r)$ is related to $h(r)$ by the Ornstein–Zernike equation. $E(r)$, called the *bridge function*, represents the sum of an infinite number of terms, the so called *elementary* graphs in the diagrammatic analysis of the two-point function. The exact bridge function is not known for any system. However, for a fluid of hard spheres an approximate bridge function can be obtained by resorting to known parametrizations of $g(r)$. Therefore, in the MHNC scheme the bridge function of the system with potential $v(r)$ is replaced by the bridge function $E_{HS}(r)$ of a fluid of hard spheres of suitable diameter d. To optimize the choice of the hard-sphere bridge function, which depends on the parameter d, the free energy is minimized [37]; this request is satisfied when

$$\int d\mathbf{r}\, [g(r) - g_{HS}(r, \eta_{HS})]\,\frac{\partial E_{HS}(r, \eta_{HS})}{\partial \eta_{HS}} = 0. \tag{10}$$

Here $\eta_{\mathrm{HS}} = \frac{\pi}{6}\rho d^3$. In order to obtain E_{HS}, we utilized the Verlet and Weis (VW) [23] parametrization of the rdf $g_{\mathrm{HS}}(r)$ of the hard-sphere fluid, based on the Percus–Yevick (PY) equation with a correction which incorporates thermodynamical consistency through the Carnahan–Starling state equation [36]. This together with equations (9), (10) gives a closed set of equations which are solved by a standard iterative method.

3. Nonadditive HS mixtures

3.1. Introduction

Consider a binary system of HS with distances of closest approach $\sigma_{\alpha\beta}$ ($1 \leqslant \alpha, \beta \leqslant 2$) such that $\sigma_{11} = \sigma_1$ and $\sigma_{22} = \sigma_2$, where subscripts 1 and 2 denote species 1 and 2 and

$$\sigma_{12} = \tfrac{1}{2}(\sigma_{11} + \sigma_{22})(1 + \Delta), \tag{11}$$

where the nonadditivity parameter Δ can be positive or negative, the case $\Delta = 0$ corresponding to additive HS. For a fixed number density ρ_2 of the small spheres, the nonadditivity can be introduced in two ways: fixing σ_{12} and varying Δ by changing the small-particle diameter, or fixing the small-particle hard-core diameter and varying Δ by changing σ_{12}. Notice that in the first case [7], on increasing the positive nonadditivity, the repulsive 'bump' at long r, r being the distance between two big spheres in solution, decreases and the potential tends toward the ideal Asakura–Oosawa limit. In this case the contact value remains relatively constant. In contrast, on increasing negative nonadditivity the contact value increases markedly, leading to strongly repulsive interactions. In the second case the dominant effect on depletion pair potentials is to shift them along r [7]; both positive and negative nonadditivity change the well depth at contact significantly. Indeed, changing σ_{12} changes the depletion layers of the two big particles and then the amount of volume doubly excluded when two big particles approach each other.

In this section we concentrate on positive nonadditivity, introduced in the second way. According to the procedure proposed by Louis *et al* [7], nonadditivity can be used to mimic further interactions between asymmetric spheres with respect to the depletion one, by mapping the effect of this extra interaction onto an effective nonadditive HS diameter. To obtain the effective HS diameter, the well known Barker–Henderson approach or a similar procedure can be used [38]. We then decided to search for a suitable theoretical method to study extensively the phase diagram of these asymmetric HS mixtures for very different size ratios and for different values of the nonadditivity parameter. In particular, we started from a description of this system in terms of a pair interaction as discussed in [5, 13]. The procedures used in the above-mentioned reference have been generalized by Louis *et al* to derive an effective pair potential between large spheres in a nonadditive mixture [4]:

$$\beta v_{\mathrm{eff}}(r) = \begin{cases} \infty & r < \sigma_1 \\ \dfrac{-3\eta_2^{\mathrm{r}}(1+q_{\mathrm{eff}})}{2q^3}\left\{h(r)^2 + \eta_2^{\mathrm{r}}[4h(r)^2 - 3qh(r)] \right. & \\ \qquad \left. + (\eta_2^{\mathrm{r}})^2[10h(r)^2 - 12qh(r)]\right\} & \sigma_1 \leqslant r \leqslant \sigma_1(1+q_{\mathrm{eff}}) \\ 0 & r > \sigma_1(1+q_{\mathrm{eff}}) \end{cases} \tag{12}$$

where η_2^{r} is the packing fraction of the small spheres in the reservoir, the effective size ratio q_{eff} is related to the size ratio $q = \sigma_2/\sigma_1$ by $q_{\mathrm{eff}} = q + \Delta + \Delta q$, and the function $h(r)$ is given by $h(r) = (1+q_{\mathrm{eff}}) - r/\sigma_1$. The term linear in η_2^{r} is the purely attractive Derjaguin form of the Asakura–Oosawa potential with effective size ratio q_{eff}, while the higher-order terms describe the partially repulsive effects of the correlation-induced layering of the small spheres around

the large spheres. Increasing Δ at fixed η_2^r deepens the attractive well, while the correlation-induced repulsive barrier remains approximately the same. Notice that this treatment is based on an approximation for the depletion potential; i.e. a truncated virial expansion of the Derjaguin approximation to the depletion potential for additive HS mixtures [39] is employed with an effective size ratio $q_{\rm eff} = q(1 + \Delta) + \Delta$ to take into account the nonadditivity.

Starting from this expression, by employing an effective one-component perturbation theory Louis *et al* calculated the fluid–solid coexistence curves for $q = 0.2$ and several values of Δ. Moreover, they calculated the fluid–fluid spinodal curves for the same value of the parameters using a two-component perturbation theory, where the perturbation $v_{12}^{\rm HS}[r/(1+\lambda\Delta)]$ is the hard-sphere potential between species 1 and 2 with a coupling parameter λ which varies from zero to unity so as to switch on the nonadditivity. The spinodal curve for $q = 0.2$ and $\Delta = 0.033$ agrees nicely with that given by an approximate equation of state due to Barboy and Gelbart [40], and is consistent with the result of the numerical solution of the Ballone–Pastore–Galli–Gazzillo (BPGG) [41] integral equation, at least for low values of η_1. Both of these approaches are not based on an effective potential for the one-component system, but refer directly to the two-component hard-sphere mixture. It has been shown that even a small degree of positive or negative nonadditivity can change the global topology of the phase diagram.

In [14] Dijkstra, by performing Gibbs ensemble MC simulations of the true mixture for a size ratio $q = 0.1$ and varying degrees of nonadditivity, showed the existence of a fluid–fluid demixing transition in binary nonadditive asymmetric mixtures. She also compared the results with the theoretical binodals obtained from the equation of state proposed by Barboy and Gelbart [40]. It is found that there is reasonable quantitative agreement for sufficiently large values of nonadditivity parameter, $\Delta \gtrsim 0.3$. Upon decreasing the nonadditivity both the theoretical results and, to a larger degree, the simulation ones show that the fluid–fluid phase transition shifts to higher pressures and becomes narrower; for sufficiently small nonadditivity the fluid–fluid demixing is not present, at least at packing fractions low enough for the fluid phases to be actually stable against freezing.

In the next two subsections we present our investigation of the system described by the effective pair interaction (12).

3.2. MHNC results

A first analysis of the demixing transition has been performed by using the MHNC closure. In figure 1 some results obtained by this method are shown, namely the spinodal curves for a size ratio $q = 0.2$ and several values of the nonadditivity parameter ($\Delta = 0.25, 0.2, 0.1$). Notice that on increasing the nonadditivity parameter for a fixed value of the packing fraction of the small spheres, the width of the well potential and its depth increase, i.e. the strength of the depletion force increases. Conversely, the height of the bump in the repulsive potential remains the same and it only moves toward higher r-values. These properties can be inferred from figures 2–4. In the figures we show the interaction potentials corresponding to the q and Δ values of the three curves in figure 1. The parameter η_2^r for each curve is chosen to be in the neighbourhood of the critical value.

As shown by the spinodal curves, the critical packing fraction for the big spheres is approximately stable with respect to a change in the nonadditivity parameter, whereas the critical packing fraction for the small spheres increases by reducing the nonadditivity parameter. As a side remark, we notice that the curves look rather flat and wide.

We have compared our results with the predictions by Louis *et al* [4], who determined the spinodal curves of nonadditive HS mixtures for a given value of q, $q = 0.2$, and a set of

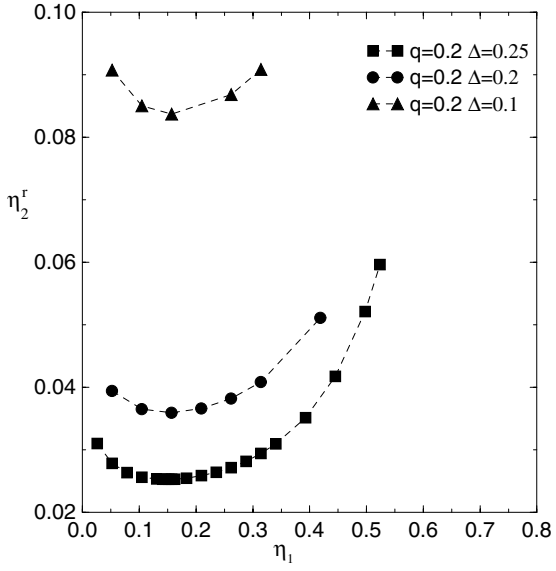

Figure 1. Spinodal curves (η_2^r versus η_1) as obtained from the MHNC integral equation for $q = 0.2$, $\Delta = 0.25$, 0.2, 0.1. Lines are simply guides to the eye.

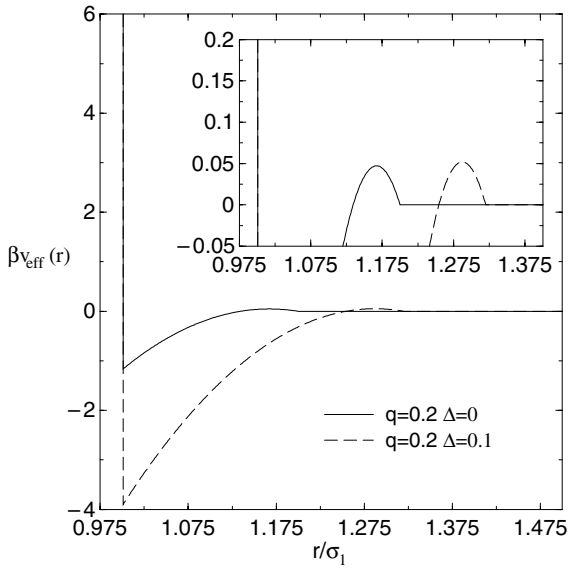

Figure 2. Effective big-sphere pair potential of a binary hard-sphere mixture with size ratio $q = 0.2$, $\eta_2^r = 0.12$, $\Delta = 0, 0.1$.

Δ values by the two-component perturbation theory mentioned in section 3.1. The qualitative behaviour of the spinodal curves as a function of the nonadditivity parameter Δ shown in figure 1 is similar to that of figure 2 in [4]. A quantitative comparison is shown in figures 5 and 6 for $\Delta = 0.25$ and 0.1 respectively. In both cases, the MHNC with the effective two-body potential (12) gives critical values for η_1 and η_2^r that are lower than those given by two-component perturbation theory. The MHNC spinodals are also considerably flatter and wider. Although additive mixtures will not be discussed in this paper, we remark that in the case of additive hard-sphere systems we found a similar trend of the MHNC result with respect to simulation predictions by Dijkstra *et al* [5], i.e., an underestimation of η_1 and η_2^r at the critical point. We have to remark that this is not a definitive test of the accuracy of MHNC

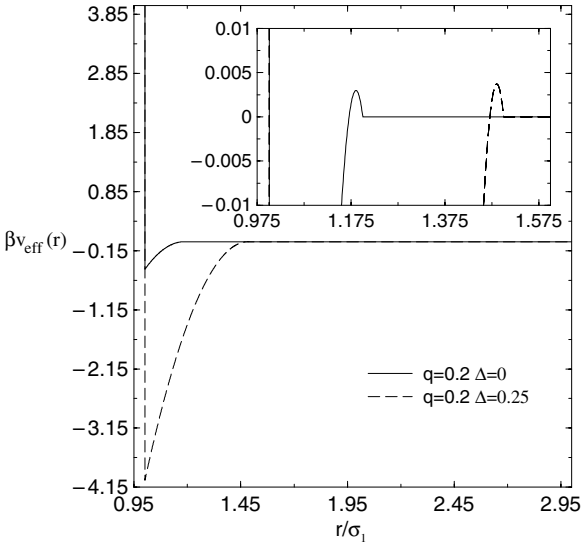

Figure 3. Effective big-sphere pair potential of a binary hard-sphere mixture with size ratio $q = 0.2$, $\eta_2^r = 0.05$, $\Delta = 0, 0.25$.

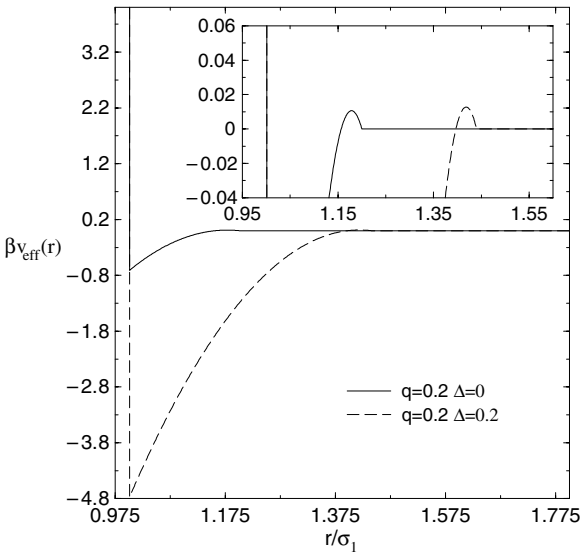

Figure 4. Effective big-sphere pair potential of a binary hard-sphere mixture with size ratio $q = 0.2$, $\eta_2^r = 0.075$, $\Delta = 0, 0.2$.

to study very narrow potentials due to the approximate character of the theory utilized in [4]. To have a definitive, conclusive check we would like to compare our MHNC results both to MC simulations and HRT. The comparison with HRT results is presented in the next section.

3.3. HRT results

HRT has been applied to the potential $v_{\rm eff}(r)$ in order to obtain the fluid–fluid and the fluid–solid phase diagrams as well as to have precise quantitative information concerning the stability of the fluid–fluid coexistence curve with respect to freezing as Δ is changed.

For the systems considered here, fluid–fluid coexistence occurs for values of η_2^r larger than the critical value η_{2c}^r. The curves at constant η_2^r correspond to the isotherms of a thermal system. We recall that HRT gives the correct convexity of the free energy even in the presence

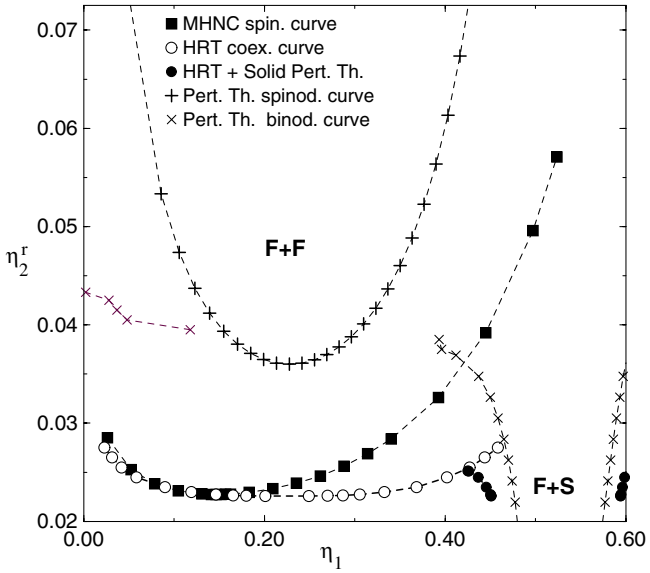

Figure 5. Fluid–fluid (HRT) and fluid–solid (HRT and solid perturbation theory) transition lines of a nonadditive hard-sphere mixture, $q = 0.2$, $\Delta = 0.25$. In the figure we also present our MHNC integral equation results for the spinodal curve and the results obtained by Louis *et al* [7] by means of perturbation theory.

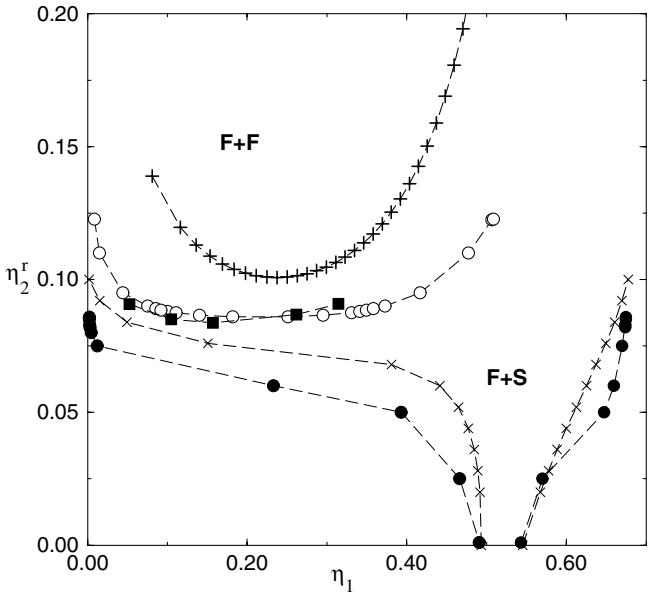

Figure 6. Fluid–fluid (HRT) and fluid–solid (HRT and perturbation theory) transition lines of a nonadditive hard-sphere mixture, $q = 0.2$, $\Delta = 0.1$. In the figure we also present a few MHNC integral equation results for the spinodal curve and the results obtained by Louis *et al* [7] by means of perturbation theory. The legend is the same as in figure 5.

of phase coexistence [42]. The unstable region of negative compressibility is suppressed by the inclusion of long-wavelength fluctuations. As a consequence, the 'isotherms' in the pressure–

Table 1. Critical values of the packing fraction of the big spheres η_1 and of the small spheres in the reservoir η_2^r for $q = 0.2$ and two different values of the nonadditivity parameter Δ for the model potential (12). In the case of stability of the fluid–fluid phase transition we also calculate the value of the packing fraction of the triple point η_{2t}^r and η_{1t}.

Δ	$\eta_2^{r,crit}$	η_1^{crit}	η_{2t}^r	η_{1t}
0.25	0.025	0.225	0.028	0.421
0.1	0.086	0.219	—	—

density plane do not display the van der Waals loop characteristic of mean-field theory, but a rigorously flat interval which immediately gives the amplitude of the coexistence region. Similarly, in the pressure–chemical potential plane, the isotherms do not show any 'bow', but the high- and low-density branches of the curve for fixed η_2^r end at their intersection point, which satisfies the condition of mechanical and chemical equilibrium between the coexisting phases. As far as the fluid–solid transition is concerned, for any given value of η_2^r we first found the values of the pressure P and chemical potential μ at coexistence by determining the intersection of the fluid and solid branches of the equation of state in the P–μ plane, and then obtained the corresponding packing fractions η_1^f, η_1^s on each branch. As specified in section 2.2, the pressure and chemical potential of the solid were determined by thermodynamic perturbation theory. Unlike HRT, this approach does not ensure the convexity of the free energy as a function of the density. In fact, for the lowest packing fractions η_1 that we considered on the solid branch, the compressibility of the solid may become negative. This unphysical part of the solid branch was removed before determining the intersection with the fluid one.

In figure 5 we present the fluid–fluid and fluid–solid coexistence curve, η_2^r versus η_1, as obtained from HRT with the core condition for $\Delta = 0.25$ and $q = 0.2$. In this case the fluid–fluid phase transition is stable with respect to the fluid–solid one. In figure 6 we present the phase diagram calculated by means of HRT for a case in which the fluid–fluid transition is metastable with respect to freezing, namely $\Delta = 0.1$, $q = 0.2$. By comparing these results with the MHNC data for the spinodal curve already presented in section 3.2, we see that in both cases the MHNC spinodal qualitatively locates the coexistence region, but it underestimates the critical packing fraction η_{1c} of the big spheres with respect to HRT. On the other hand, the critical packing fraction η_{2c}^r of the small spheres in the reservoir is in close agreement with that of HRT.

In both of the cases investigated, the HRT prediction about the stability ($\Delta = 0.25$) or metastability ($\Delta = 0.1$) of the fluid–fluid transition with respect to freezing is in agreement with the results of Louis *et al* [4], also reported in the figures. However, considerable quantitative differences appear. In table 1 we showed the critical values of the packing fraction of the big spheres and small spheres in the reservoir for $q = 0.2$ and two different values of Δ. The HRT value of η_{2c}^r is 25% ($\Delta = 0.1$) and 50% ($\Delta = 0.25$) smaller than that of [4]. This is not very surprising, in view of the fact that these approaches differ not only because of the different liquid-state theories employed, but also because of the different methods used to deal with the interactions of the systems: as pointed out before, in [4] the fluid–fluid transition was studied by applying perturbation theory directly to the binary mixture of nonadditive spheres, while here HRT is applied to the effective one-component fluid described by the potential (12). The same consideration holds when comparing the results of [4] with the MHNC ones reported in the previous subsection. We also note that the HRT coexistence curve is much flatter than the spinodal given by two-component perturbation theory, and we expect this also to be true if the coexistence curve predicted by the latter approach is compared to that of HRT. In fact, in mean-field theories the coexistence curve close to the critical point is described by the same

'classical' critical exponent $\beta = 0.5$ as the spinodal, while HRT gives a value of β which is smaller than the classical result, and in much better agreement with the generally accepted value $\beta \simeq 0.324$ (see section 4.3).

As a further check of our results, we compared the HRT prediction for the fluid–fluid critical point with the MC simulation by Dijkstra *et al* [14] of a binary hard-sphere mixture for a size ratio $q = 0.1$ and varying degree of nonadditivity. As we said in the introduction, the authors compared these results with the theoretical binodals obtained from the equation of state proposed by Barboy and Gelbart [40]. We then determined via HRT the values of the total critical packing fraction of the big and small spheres, η_{T_c} (i.e., $\eta_{T_c} = \eta_{2c} + \eta_{1c}$) for $q = 0.1$ and $\Delta = 0.3, 0.4, 0.5$, and compared them with the results presented in [14]. We found that the HRT results for η_{T_c}, not reported here, appear nearly independent of Δ, unlike the MC and Barboy–Gelbart predictions. It is likely that this discrepancy should be at least partially traced back to the fact that, unlike HRT, both the MC simulations and the calculations based on the Barboy–Gelbart equation were performed on the two-component mixture rather than on the one-component fluid with an effective potential.

4. An extreme case of nonadditivity: the Asakura–Oosawa model

4.1. Introduction

It is well known that the addition of polymer to a suspension of spherical colloids can cause an effective attraction between particles [43]. A very simple model for this situation was proposed by Asakura and Oosawa [44] (AO model) and independently by Vrij [45]. The AO model represents an extreme case of nonadditivity. In this model the polymers are assumed to be noninteracting, freely interpenetrable coils with a radius of gyration R_g much smaller than the size of the colloidal particles. The polymer–polymer interaction is zero. However, they are excluded from the colloids to a certain centre-of-mass distance σ_{cp}. Therefore, with respect to their interaction with colloidal particles of radius $\sigma_c/2$, the polymer molecules are assumed to behave as hard spheres of radius $\sigma_p/2 = R_g$, the diameter of the colloid–polymer interaction being $\sigma_{cp} = (\sigma_c + \sigma_p)/2$. A simple expression results for the effective (pair) interaction of hard-sphere particles in the presence of added free polymer:

$$\beta v_{AO}(r) = \begin{cases} \infty & r < \sigma_c \\ -\dfrac{\pi\sigma_p^3 z_p}{6}\dfrac{(1+q)^3}{q^3}\left[1 - \dfrac{3r}{2(1+q)\sigma_c} + \dfrac{r^3}{2(1+q)^3\sigma_c^3}\right] & \sigma_c < r < \sigma_c + \sigma_p \\ 0 & r > \sigma_c + \sigma_p \end{cases} \tag{13}$$

where z_p is the fugacity of a pure ideal polymer system and $q = \sigma_p/\sigma_c$. The origin of the attraction outlined above has been called 'volume restriction' or 'osmotic depletion', and the resulting force 'depletion force'. Notice that, for given z_p and q, the strength of the attractive interaction is proportional to the volume of the intersection region among the shells of excluded volume for the colloidal spheres. Simple geometrical arguments show that for $q = \frac{\sigma_p}{\sigma_c} < 0.154$ three-body and higher-body terms are equal to 0 [28]. For larger values of the size ratio, a multiple overlap of the depletion zones is possible, and consequently the interaction also presents many-body terms. In spite of its simplicity, the effective pair potential of equation (13) captures the main features of the experimental phase diagrams of polymer–colloid mixtures, namely the disappearance of fluid–fluid phase separation into the fluid–solid coexistence region for small values of the polymer–colloid size ratio q [46]. As q is increased and the depletion potential becomes longer ranged, a stable fluid–fluid phase transition occurs [28, 47, 48].

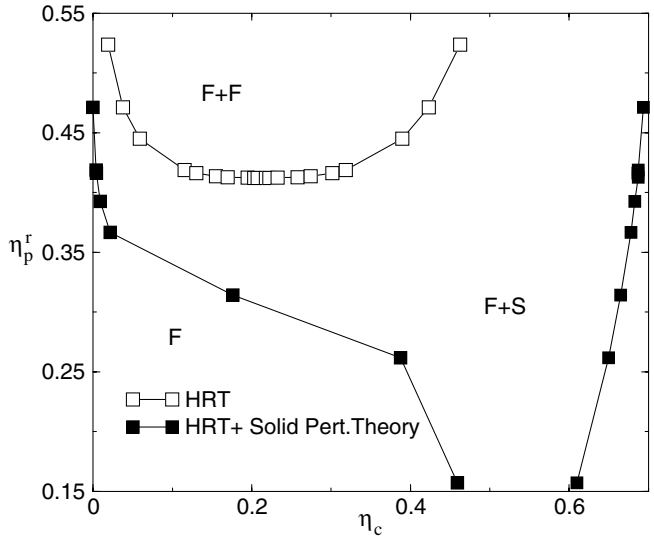

Figure 7. Fluid–fluid (HRT) and fluid–solid (HRT and perturbation theory) transition lines of a colloid–polymer mixture described by means of the AO pair interaction ($q = 0.25$).

If we consider the general equation (11) for nonadditive mixtures, the AO model corresponds to $\sigma_{22} = 0$ and $\Delta = q$. However, we remark that in this limit the effective potential (12) does not yield equation (13) for the AO potential. The reason for this is that equation (12) is based on the Derjaguin approximation, unlike equation (13). Therefore, in the above limit it reduces to the Derjaguin approximation for the AO potential between hard-sphere colloids.

Here we apply HRT to the two-body AO potential (13) and compare our results with those obtained by Dijkstra *et al* [12] by MC simulations and thermodynamic perturbation theory. Unlike the results discussed in sections 3.2, 3.3, these studies were performed on the same potential v_{AO} that we considered, rather than on the two-component mixture. This allows for a more direct comparison with the HRT results.

4.2. Phase diagram

We first performed HRT calculations for a small value of the size ratio, in a region where we expect the fluid–fluid phase separation to be metastable with respect to freezing. As the first case investigated we present in figure 7 the phase diagram for $q = 0.25$ in the η_p^r–η_c plane, η_p^r and η_c being respectively the reservoir packing fraction of polymer and the packing fraction of colloid. As introduced above, we calculated the fluid–solid equilibrium by supplementing HRT with thermodynamic perturbation theory for the solid phase. The metastability of the fluid–fluid coexistence curve with respect to freezing is in agreement with the trend evidenced in [12].

As the second case we calculated the phase diagram for $q = 0.4$. The HRT results agree fairly well with the simulation performed by Dijkstra *et al* [12]. From figure 8 we observe that both simulation and HRT predict a metastable fluid–fluid phase transition, unlike perturbation theory. We emphasize that HRT gives a critical point which lies slightly above the fluid–solid line. This could in principle also be the case for MC simulation, considering that there are no values of the critical packing fraction in the reservoir between $0.2 \lesssim \eta_c \lesssim 0.35$. The

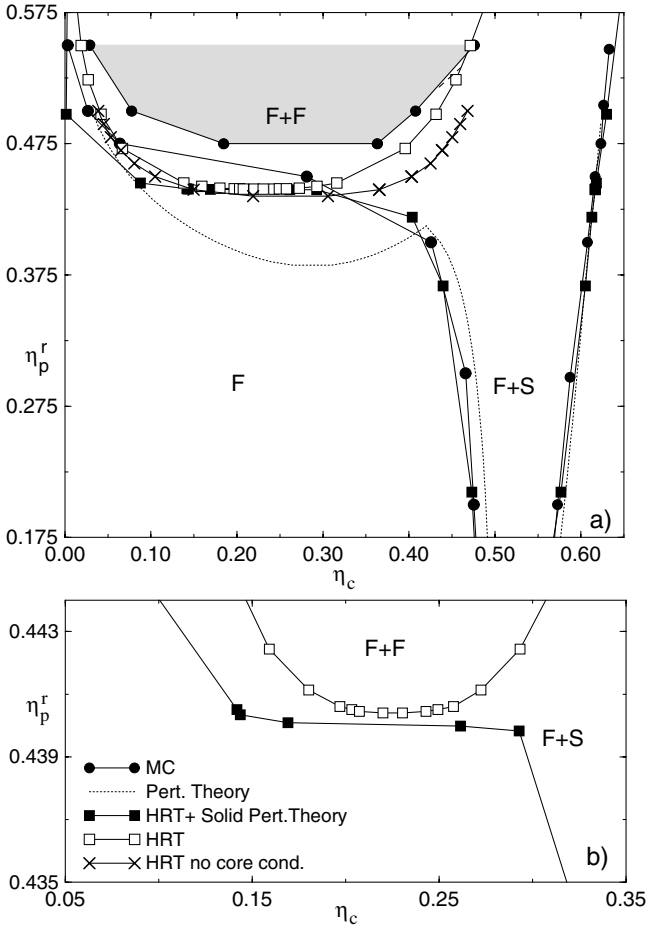

Figure 8. Fluid–fluid (HRT) and fluid–solid (HRT and perturbation theory) transition lines of a colloid–polymer mixture described by means of the AO pair interaction, $q = 0.4$ (squares). In the figure we also present HRT results on the coexistence curve calculated without the core condition (crosses). (a) We compare our results with perturbation theory results and MC simulation results by Dijkstra *et al* [12]. (b) Magnification of the region of coexistence as calculated by HRT.

difference between the HRT and the MC result for $\eta_p^{r,crit}$ is smaller than 7.5%. According to HRT, the fluid–fluid transition becomes stable just above $q = 0.4$, in good agreement with the MC results, which locate the stability threshold at $q \simeq 0.45$ [12]. If perturbation theory for both the fluid and the solid phase is used, the threshold is instead located at $q \simeq 0.31$ [12]. The crossover from metastable to stable fluid–fluid phase separation on increasing q has been observed in experiments on colloid–polymer mixtures and in simulations of hard spheres and lattice polymers [12, 46, 49, 50].

We then consider $q = 0.6$: in this case also the HRT results are in much better agreement with the simulations performed by Dijkstra *et al* [12] than the predictions of perturbation theory (see figure 9). For this value of q, simulation, perturbation theory, and HRT all give a stable fluid–fluid phase transition. However, the critical value of η_p^r predicted by HRT is considerably higher, and closer to the MC value, than that of perturbation theory, because of the inclusion of fluctuations.

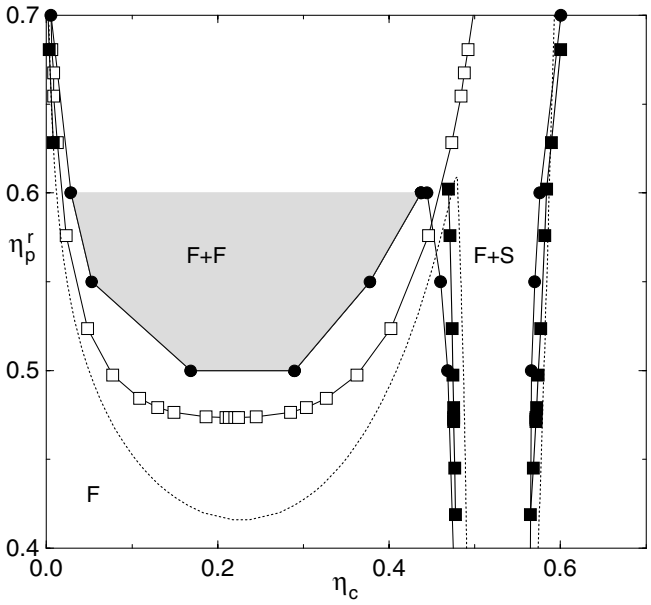

Figure 9. Fluid–fluid (HRT) and fluid–solid (HRT and perturbation theory) transition lines of a colloid–polymer mixture described by means of the AO pair interaction ($q = 0.6$). In the figure we compare our results with perturbation theory results and MC simulation results by Dijkstra *et al* [12]. Symbols as in figure 8.

In figure 10 we show the comparison between our HRT results and the simulation performed by Dijkstra *et al* [12] for $q = 0.8$. Also in this case the agreement for the fluid–fluid transition is very good. On the other hand, the curve obtained via perturbation theory differs appreciably from HRT and MC simulation results. We must point out that, for this value of q, we were not able to determine the fluid–solid equilibrium lines for the range of η_p^r shown in the figure, because the fluid and solid branches of the equation of state as given by HRT and perturbation theory respectively did not cross in the P–μ plane, at least for the version of perturbation theory used here, where the second-order term was estimated by equation (8). We did not try to improve the accuracy of the perturbation theory calculation so as to recover the freezing transition, since we were interested in this relatively large value of q mainly in connection with the critical behaviour of the fluid–fluid transition discussed in the next subsection.

Finally, in table 2 we showed the critical values of the packing fractions of the big spheres and small spheres in the reservoir for $q = 0.25, 0.4, 0.6, 0.8$.

We can make a few remarks about all the AO cases investigated: first of all, we note that here the packing fraction of the small spheres in the reservoir has the same role as an inverse temperature. In the case of a Lennard-Jones potential, the effect of fluctuations as embodied in HRT gives a lower value of the critical temperature with respect to the mean-field approach (MF). Therefore, in this case it gives a value of $\eta_p^{r,crit}$ higher than the mean-field one. Moreover, HRT gives a coexistence curve very flat compared to the MF results. The curves obtained by means of MC simulation do not present enough points in the critical region to be a relevant term of comparison about the curvature of the coexistence curve. We will consider this point in more detail in the next section. Second, we observe from the figures that the critical packing fraction of polymers in the reservoir increases on increasing the size ratio q, while the critical

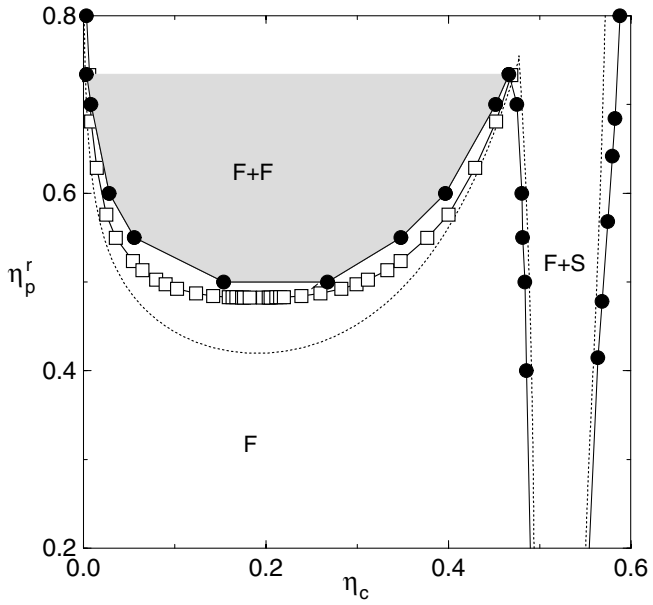

Figure 10. Fluid–fluid (HRT) and fluid–solid (HRT and perturbation theory) transition lines of a colloid–polymer mixture described by means of the AO pair interaction ($q = 0.8$). In the figure we compare our results with perturbation theory results and MC simulation results by Dijkstra *et al* [12]. Symbols as in figure 8.

Table 2. Critical values of the packing fraction of the big spheres η_c and of the small spheres in the reservoir η_p^r of the AO model for a diameter ratio $q = 0.25, 0.4, 0.6, 0.8$. For $q = 0.6$ we also calculate the value of the packing fraction of the triple point η_{2t}^r and η_{1t}. The triple point for $q = 0.8$ is not shown because for this value of q we were unable to locate the freezing transition by the solid perturbation theory described in the text.

q	$\eta_p^{r,crit}$	η_c^{crit}	$\eta_p^{r,t}$	η_c^t
0.25	0.4123	0.213	—	—
0.4	0.4404	0.225	—	—
0.6	0.4736	0.216	0.617	0.467
0.8	0.4825	0.190		

packing fraction of colloids does not change very much as a function of q. Third, we point out that the agreement between HRT results and MC simulations is good overall and that HRT significantly improves over perturbation theory. However, the discrepancies between HRT and simulation data are larger than those found in previous investigations on the Lennard-Jones potential [22], especially as the polymer–colloid size ratio q decreases. This should be traced back to the fact that, as stated in section 2.1, the approximate closure for the correlations that we used in our HRT calculation is more appropriate for Lennard-Jones-like potentials rather than for the short-ranged, strongly attractive forces typical of depletion interactions. In fact, even for the largest diameter ratio that we considered, namely $q = 0.8$, the profile of the AO potential is quite different from that expected for a simple atomic fluid. In figure 11 we compare the AO potential for $q = 0.8$ to a Yukawa potential $v_{yuk}(r) = -\epsilon \exp[-z(r-1)]/r$ with an inverse-range parameter $z = 1.8$, which is an appropriate value to mimic a Lennard-Jones-like interaction. The polymer packing fraction η_p^r of the AO potential and the temperature of the

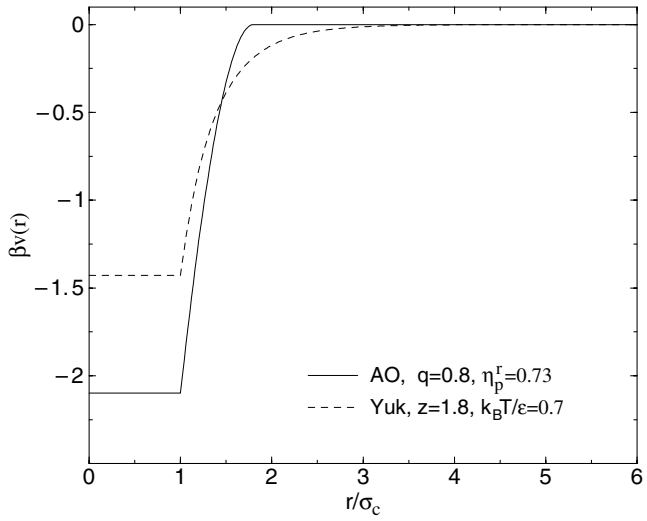

Figure 11. Comparison between the AO potential for $q = 0.8$ and the Yukawa potential with an inverse-range parameter $z = 1.8$, which is an appropriate value to mimic a Lennard-Jones-like interaction. The values of the polymer packing fraction $\eta_{\mathrm{p}}^{\mathrm{r}} = 0.73$ and the reduced temperature $k_{\mathrm{B}}T/\epsilon = 0.7$ both refer to triple-point conditions.

Yukawa potential have been set so as to be close to triple-point conditions. We checked that the integrated intensities of the interactions are nearly the same in the two cases. However, the AO interaction is much deeper and narrower. This statement can be made more quantitative by considering two definitions of the potential range recently proposed in the literature in order to give this parameter an unambiguous meaning even for different interaction profiles. In [51], Noro and Frenkel introduced a reduced temperature and a reduced second virial coefficient by rescaling the temperature T and the second virial coefficient $B_2(T)$ by the depth of the attractive potential well and by the hard-sphere value of B_2 respectively, and proposed to define the potential range as the width δ of the square-well potential which gives the same reduced B_2 at the same reduced T as the original potential. The range thus obtained depends on the temperature or, for the depletion interaction considered here, on η_2^{r}, since this parameter affects the depth of the attractive well. A different prescription was adopted by Louis [52] on the basis of the *isosbestic points*, i.e., values of the wavevector k such that, for a given interaction, the structure factor at fixed density is approximately left unaltered in a wide temperature interval. Louis suggested to identify the potential range as the amplitude δ of the square-well potential whose smallest isosbestic point, in units of the reciprocal of the hard-sphere diameter, coincides with that of the interaction in hand. According to both of these prescriptions, for the parameter choice corresponding to figure 11, the range of the Yukawa potential is nearly twice that of the AO potential. This feature is bound to affect the accuracy of the closure that we used in our HRT calculation, especially for smaller values of q. In this respect, it is particularly important to recall that for hard-core potentials which contain deep and narrow attractive wells the requirement that the particles do not overlap because of the excluded-volume effect is expected to play a more important role than in interactions with smooth, longer-ranged tails. As an example, in figure 8 we have also plotted the fluid–fluid coexistence curve predicted by HRT when the core condition is disregarded altogether: this considerably deviates from the MC simulation data, especially as far as the high-density branch is concerned. Therefore, imposing the core condition clearly improves our results. However, we must point out that

in the closure currently adopted within HRT such a condition has been implemented in an approximate fashion, and that the approximations involved are bound to become less and less accurate as the interaction becomes more sticky. In fact, we found that for very small values of the size ratio, namely $q \lesssim 0.2$, our HRT calculation failed to converge before the occurrence of fluid–fluid phase separation. The limits of this treatment also clearly appear in the two-body correlations: as the polymer packing fraction η_p^r increases, we found that not only is the core condition poorly satisfied, but the overall profile of the radial distribution function $g(r)$ shows appreciable discrepancies with respect to both MC results [12] and the predictions of integral-equation theories such as PY [12] and MHNC. Improving the core condition within HRT is a nontrivial matter, but some preliminary investigations show that this is indeed possible, and will not only increase the accuracy of the correlations, but also give even better phase diagrams and thermodynamics. We propose to report on these developments in the future.

Experiments on the phase behaviour of sterically stabilized polymethylmethacrylate and nonadsorbing polystyrene in decalin show a trend similar to that of the AO potential [12, 46]. However, the experimental value $q \lesssim 0.25$ of the metastability threshold is rather lower than the value $q \lesssim 0.4$ of the AO potential obtained by HRT as well as by MC simulations by Dijkstra *et al* [12]. A possible source of the discrepancy might be the presence of many-body terms not accounted for in the AO potential. As the diameter ratio q increases, these contributions to the effective interaction between colloidal particles strongly affect the phase diagram of the mixture: by comparing the MC results by Vink *et al* [17] for the AO mixture with $q = 0.8$ to those previously obtained for the purely two-body potential equation (13) [12], it appears that disregarding many-body contributions leads to an underestimation of the critical polymer packing fraction $\eta_p^{r,crit}$ of nearly 40%. On the other hand, the free-volume approach which incorporates some many-body effects, as discussed in [12], predicts a value of the metastability threshold higher than the experimental one, while direct simulations of a lattice model of the AO interaction estimate the value of crossover near 0.45 [50]. Other features of real systems which are not taken into account in the AO model include the nonideality or deformability of the polymers and the polydispersity of the colloids and polymers. These effects are the object of many investigations. In any case, we emphasize that the main purpose of the present work is to test the ability of HRT to describe the phase behaviour of asymmetric, nonadditive hard-sphere mixtures starting from very simple models of the pair interaction, which have already been extensively studied by simulation and other liquid-state approaches. In order to compare our results directly with experiments, more accurate forms of the effective interaction will have to be employed.

4.3. Critical fluctuations

The critical behaviour of colloid–polymer mixtures has not received much attention so far. Lately, this issue has been investigated by accurate finite-size scaling Monte Carlo studies of the two-component AO model with a diameter ratio $q = 0.8$ [16, 17], which give evidence that this system belongs to the Ising universality class. We remark that within the description adopted here, where the two-component mixture is replaced by a one-component fluid with the two-body potential (13), the critical behaviour is necessarily the same as that of a simple fluid, provided the inverse temperature is replaced by the fugacity z_p (or, equivalently, the packing fraction η_p^r) of the polymer in the reservoir as the criticality-driving field. Therefore, Ising criticality is to be expected if the effective-potential description is adopted. We recall that in thermal binary mixtures, which also belong to the Ising universality class, the critical exponents are generally 'renormalized' with respect to their usual Ising values by a factor $1/(1-\alpha)$ [53]. On the other hand, we do not expect exponent renormalization to occur in the case considered

here. In fact, as pointed out above, the two-body potential (13) describes exactly the interactions between colloidal particles for polymer-to-colloid size ratio $q < 0.154$. Therefore, in this regime the colloid will certainly display standard Ising-like critical behaviour, if η_r^p is used as the thermal field. More generally, in thermal binary mixtures exponent renormalization comes along as a consequence of Fisher's assumption [53], according to which the singular part of the grand potential per unit volume ω of the binary fluid can be expressed via the corresponding quantity ω_0 of the one-component fluid as $\omega(\mu_1, \mu_2, T) = \omega_0(T^*(\mu_1, \mu_2, T), \mu^*(\mu_1, \mu_2, T))$, where the 'effective' temperature T^* and chemical potential μ^* are analytic functions of the temperature T and chemical potentials μ_1, μ_2 of the two species. However, the AO model is an athermal system, so that in the above expression the temperature is absent, and its role is played by one of the chemical potentials. This form of ω is not expected to give exponent renormalization since, in terms of Fisher's original formulation, there is no 'hidden' field left.

We now consider the HRT results for the critical behaviour of the AO model. It is worthwhile recalling that HRT yields nontrivial values for the critical exponents. Within the present formulation of HRT, the exponents are correct up to first order of the expansion in powers of $\epsilon = 4 - d$, d being the dimensionality of the system [15]. Higher orders of the expansion are not correctly reproduced, because equation (4) implies that the direct correlation function in momentum space is an analytic function of the wavevector k even at the critical point, $\mathcal{C}_Q(k) \sim k^2$, thereby setting the critical exponent η to zero. Even so, the description of criticality is considerably more accurate than that of thermodynamic perturbation theory and integral-equation approaches. First, we compare the HRT coexistence curve for $q = 0.8$ with the finite-size scaling results by Vink *et al* [16] for the same value of q. These authors simulated the true two-component AO model, thereby taking many-body contributions into account. As a consequence, as observed in section 4.2, the location of the critical point differs considerably from that of the purely two-body interaction, equation (13). Specifically, the HRT prediction for the critical point is $\eta_{\rm p}^{\rm r,crit} = 0.483$, $\eta_{\rm c}^{\rm crit} = 0.190$, while the finite-size scaling analysis of the AO binary system gives $\eta_{\rm p}^{\rm r,crit} = 0.766$, $\eta_{\rm c}^{\rm crit} = 0.134$ [17]. However, this is not expected to affect the universal features of the transition. We then compared our results for the coexistence curve to those of [16] by using reduced quantities in both cases. Figure 12 shows an enlargement of the critical region on a log–log scale. The HRT results for the difference of the reduced densities of the colloid on the 'liquid' and 'vapour' branches of the coexistence curve $M = (\eta_{\rm c}^{\rm l} - \eta_{\rm c}^{\rm v})/(2\eta_{\rm c}^{\rm crit})$ as a function of the reduced 'temperature' $t = (\eta_{\rm p}^{\rm r} - \eta_{\rm p}^{\rm r,crit})/\eta_{\rm p}^{\rm r,crit}$ are compared with the asymptotic power law $M \sim A\, t^{\beta}$ obtained from finite-size scaling. The critical exponent β of the finite-size scaling analysis coincides with the generally accepted value $\beta = 0.324$ for the Ising universality class in three dimensions [16]. A linear fit of our results in the range $-5 \lesssim \log(t) \lesssim -4$ gives a power-law behaviour with $\beta = 0.37$. The asymptotic value of the exponent β predicted by HRT has been obtained by linearizing the renormalization-group flow induced by the HRT evolution equation (3) in the neighbourhood of the critical point and is given by $\beta = 0.345$ [15].

In figure 13 we consider the behaviour of the reduced compressibility $\chi_{\rm red}$ of the colloid on the critical isochore in the one-phase region. As before, we report both the HRT results and the asymptotic power law obtained from finite-size scaling, $\chi_{\rm red} \sim B|t|^{-\gamma}$, $\gamma = 1.239$ [16]. The HRT asymptotic value for γ is $\gamma = 1.378$, about 10% larger than the correct one [15]. A linear fit of the data shown in the figure in the range $-5.5 \lesssim \log(t) \lesssim -4.5$ gives $\gamma = 1.37$. For HRT, we have also plotted the results for the correlation length ξ which governs the decay of the correlations near the critical point. The divergence of ξ on the critical isochore asymptotically close to the critical point is described by a critical exponent ν according to the power law $\xi \sim C|t|^{-\nu}$. As recalled above, the current implementation of HRT necessarily gives a vanishing critical exponent η. Therefore, the critical exponent relation $\gamma = (2 - \eta)\nu$ becomes just $\nu = \gamma/2$.

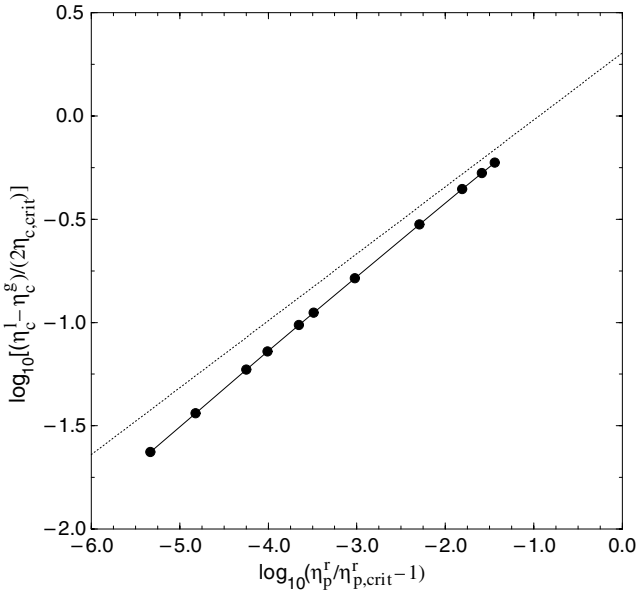

Figure 12. Coexistence curve of the AO model for $q = 0.8$ in the critical region. The quantities η_c^l and η_c^g are the packing fractions of the colloid on the high- and low-density branch of the coexistence curve respectively. Solid curve and full circles: HRT results for the AO fluid with the two-body potential (13). Dotted curve: asymptotic power law for the true binary AO mixture determined via finite-size scaling [16].

We point out that the HRT results in the critical region shown here contain no free parameters. Therefore, we regard the agreement with the asymptotic power-law behaviour obtained from finite-size scaling as quite satisfactory. On the other hand, while the power-law exponents are universal, the amplitudes are not, and are expected to be affected by many-body terms which are disregarded in the effective one-component description. Therefore, a more cogent test of the HRT would require simulations in the critical region for a smaller value of q, such that many-body terms are less important.

It is interesting to compare the HRT results for the reduced compressibility and the correlation length of the AO fluid with the corresponding quantities for the LJ-like hard-sphere Yukawa potential with inverse range $z = 1.8$ shown in figure 11. For the latter interaction, the crossover region from mean-field to Ising-like critical behaviour is appreciably larger than for the AO potential: for instance, a linear fit on a log–log scale for the compressibility of the Yukawa fluid in the same reduced temperature range as used for the AO fluid gives $\gamma = 1.36$, which is farther from the HRT asymptotic value than the AO result. Similarly, the deviation of the log–log plot from linearity is stronger for the Yukawa fluid. This can be more easily appreciated in the inset of figure 13, which shows the effective exponents $\gamma_{\rm eff}$, i.e., the local slope of the log–log plot of $\chi_{\rm red}$ versus t. Such a behaviour is most likely due to the longer range of the Yukawa interaction. According to a general renormalization-group result [54], this pushes the asymptotic region where Ising-like critical behaviour is observed to smaller reduced temperatures.

One of the quantities most directly accessible to experiments is the structure factor $S(k)$. This is shown in figure 14 for $\eta_c = \eta_c^{\rm crit}$ and two values of η_p^r close to $\eta_p^{r,{\rm crit}}$. For these near-critical states, changing η_p^r affects mainly the long-range structure because of the

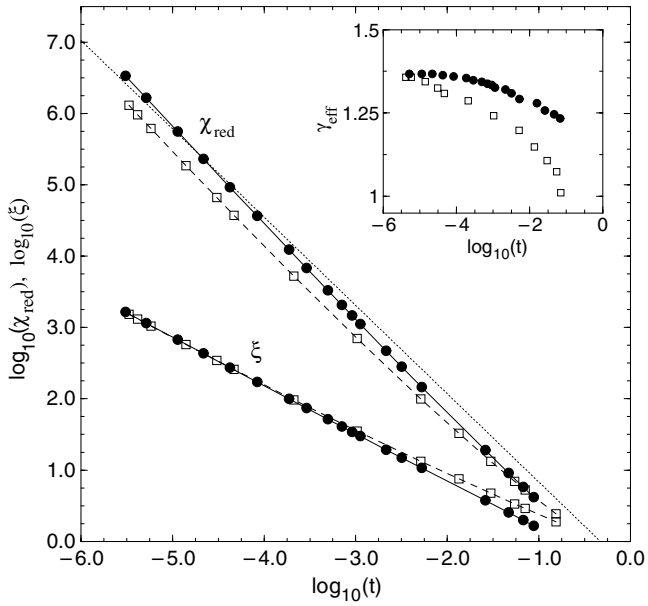

Figure 13. Reduced compressibility $\chi_{\rm red}$ (upper curves) and correlation length ξ (lower curves) for the AO fluid with $q = 0.8$ and the hard-sphere Yukawa fluid with inverse-range parameter $z = 1.8$. Solid curve and full circles: HRT results for the AO fluid with the two-body potential (13). Dashed curve and open squares: HRT results for the hard-sphere Yukawa fluid. Dotted curve: asymptotic power law for the reduced compressibility of the AO mixture determined via finite-size scaling [16]. For the AO model, the reduced temperature t is defined as $t = |\eta_{\rm p}^{\rm r} - \eta_{\rm p}^{\rm r,crit}|/\eta_{\rm p}^{\rm r,crit}$. For the Yukawa fluid, one has $t = (T - T_{\rm c})/T_{\rm c}$. Inset: effective exponent $\gamma_{\rm eff}$ according to HRT for the AO fluid (full circles) and the hard-sphere Yukawa fluid (open squares).

divergence of $\chi_{\rm red} = S(k = 0)$ at the critical point, while the short-range structure is nearly unaffected.

We conclude this section by recalling that critical fluctuations in colloidal systems are expected to play an important role even when the fluid–fluid transition is metastable with respect to the fluid–solid one as a consequence of the colloid–colloid interaction being very short ranged. In fact, it has been suggested [55] that the large density fluctuations induced by a metastable critical point can lower the free energy barrier for nucleation of the solid in the fluid phase, and therefore greatly enhance the nucleation rate. This is another situation where the ability of HRT to deal realistically with criticality might be useful.

5. Conclusions

In this paper we have considered fluids modelled by nonadditive highly asymmetric HS mixtures. The main interest of this study lies in the possibility of exploring a wide variety of attractive or repulsive generalized depletion potential shapes and associated phase behaviour, by a proper tuning of the nonadditivity. We have focused for the moment on the effect of a positive nonadditivity. In this context our main purpose is to test the hierarchical reference theory in order to identify a good theoretical tool to study the very deep and narrow attraction, characteristic of the effective interactions in these mixtures, and to describe the fluid–fluid and fluid–solid phase diagram. This theory has been especially devised to deal with the onset of long-range correlations which play a crucial role in criticality and phase separation. In this

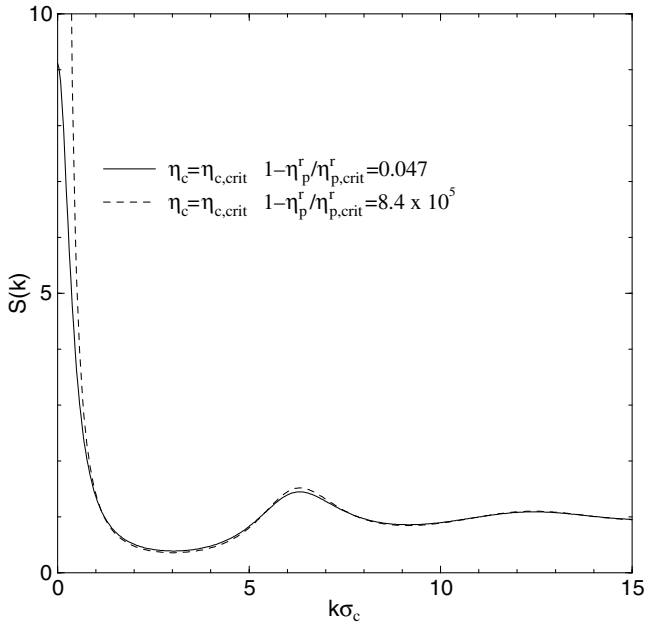

Figure 14. Structure factor of the AO fluid with the two-body potential (13) and $q = 0.8$ for two states in the neighbourhood of the critical point.

respect, it is in general more accurate than usual fluid-state theories. This is a first investigation in the possible involvement and development of HRT theory to study these deep and short-ranged interactions. Consequently, we started utilizing a one-component HRT on very simple models for the pair interaction, which anyway contain most of the features which could cause some loss of accuracy of the theory. For these simple models our results could be compared with those previously obtained in the literature, either via simulations or other theoretical approaches. As introduced above, at the present stage the expression for the correlations (4) that we used in the HRT equation is the same one that we employed for Lennard-Jones-like interactions.

First of all we studied a very general case: we considered an effective pair interaction between big particles which takes into account the interaction between the small spheres in solution, and the nonadditivity can be tuned. Our predictions for the stability or metastability of the fluid–fluid phase transition with respect to freezing are in qualitative agreement with those previously obtained in [7], where a two-component perturbation theory was used for the fluid phase.

Second, we applied HRT to the two-body AO potential equation (13) and compared our results with those found by Dijkstra *et al* [12] by MC simulations and thermodynamic perturbation theory. Both our results and those in [12] start from the same effective pair interaction between colloidal particles. We performed HRT calculations for several values of the size ratio and we found a very good agreement with simulation results. Moreover, HRT significantly improves over perturbation theory in the fluid region. Notice that the agreement increases on increasing the size ratio. This is due to the fact that the closure employed in this study is tailored to relatively long-ranged potentials.

We have to remark on some details related to our analysis: in the two cases of nonadditivity that we considered we found that it is very important to impose the core condition in the HRT scheme. However, in the closure currently adopted within HRT such a condition has been implemented by resorting to a number of approximations, which become less accurate as the

interaction becomes deeper and narrower. Actually, for very small values of the size ratio, e.g. $q \lesssim 0.2$ for the AO pair interaction, our numerical algorithm failed to converge before the occurrence of fluid–fluid phase separation. The limits of this treatment clearly appear in the two-body correlations: the current implementation of HRT does not describe the correlations at the same level of accuracy as the thermodynamics, and integral-equation approaches such as the PY [12] or the MHNC theories provide better results for the two-body radial distribution function and structure factor. In this respect, it would be interesting to compare the HRT results for the phase diagram with those of integral-equation theories. However, we remark that these theories usually suffer from a lack of solutions close to the critical point which makes available to them only a portion of the fluid–fluid phase boundary, while HRT remains convergent even arbitrarily close to the critical point. In fact, one of the most interesting features of HRT is that it gives a realistic treatment of critical fluctuations, with nonclassical values of the critical exponents and rigorously flat isotherms in the region of phase coexistence. Moreover, we stress here that the CPU time we need to calculate the fluid–fluid phase diagram with HRT is considerably small. Indeed, for a density grid of about 1000 points, a full isotherm takes less than 5 minutes on an average desktop workstation, the time scaling approximately in a linear way with the density mesh. Therefore, about 1 h CPU time is enough to obtain an accurate mapping of the coexistence curve.

We point out that here we are not interested in discussing the validity of the two-body pair interaction. Indeed, it is known that the validity of the effective pair interaction is questionable for size ratio bigger than 0.154. Rather, we are interested in checking HRT theory; for this purpose we considered the cases for which our results could be compared with available MC simulation data for the thermodynamics of the hard-sphere mixtures. A further step could be to employ a more accurate form of the pair interaction for these systems and to compare our predictions more directly with experiments. In this respect, nonadditive hard-sphere mixtures can be of interest in many different situations since, as proposed by Louis *et al* [7], nonadditivity can be used to model extra interactions between the species besides that of purely excluded volume. Before doing this, however, our next task is improving the closure relation used in HRT so as to obtain an approach which is as accurate for the correlations as it is for the thermodynamics, even in the presence of short-ranged and strongly attractive interactions. This is a work in progress.

Acknowledgments

We are grateful to Marjolein Dijkstra for sending us the MC and perturbation theory results for the phase diagram and the PY results for the correlations of the AO potential (13) presented in [12], to Adrian Louis for sending us the perturbation theory results for the phase diagram of the model potential (12) presented in [4], and to Jurgen Horbach for sending us his MC results for the phase diagram of the AO mixture prior to publication. We also thank Robert Evans for interesting conversation. Federica Lo Verso acknowledges financial support from INFM. This work is funded in part by a grant of the Marie Curie programme of the European Union, contract number MRTN-CT2003-504712.

References

[1] Wood W W and Jacobson J D 1957 *J. Chem. Phys.* **27** 1207
[2] Alder B J and Wainwright T E 1957 *J. Chem. Phys.* **27** 1208
[3] Bolhuis P G, Louis A A and Hansen J P 2002 *Phys. Rev. Lett.* **89** 128302
[4] Louis A A, Finken R and Hansen J P 2000 *Phys. Rev.* E **61** R1028
[5] Dijkstra M, van Roij R and Evans R 1999 *Phys. Rev.* E **59** 5744

[6] Belloni L 2000 *J. Phys.: Condens. Matter* **12** R549
[7] Louis A A and Roth R 2001 *J. Phys.: Condens. Matter* **13** L777
[8] Israelachvili J N 1992 *Intermolecular and Surface Forces* (London: Academic)
[9] Widom B and Rowlinson J 1970 *J. Chem. Phys.* **52** 1670
[10] Roth R, Evans R and Louis A A 2001 *Phys. Rev.* E **64** 051202
[11] Vliegenthart G A and Lekkerkerker H N W 2000 *J. Chem. Phys.* **112** 5364
[12] Dijkstra M, Brader J and Evans R 1999 *J. Phys.: Condens. Matter* **11** 10079
[13] Dijkstra M, van Roij R and Evans R 1999 *Phys. Rev. Lett.* **82** 117
[14] Dijkstra M 1998 *Phys. Rev.* E **58** 7523
[15] Parola A and Reatto L 1995 *Adv. Phys.* **44** 211
[16] Vink R L C, Horbach J and Binder K 2005 *Phys. Rev.* E **71** at press
[17] Vink R L C and Horbach J 2004 *J. Chem. Phys.* **121** 3253
Vink R L C and Horbach J 2004 *J. Phys.: Condens. Matter* **16** S3807
[18] Louis A A 2001 *Phil. Trans. R. Soc.* A **359** 939
[19] Lo Verso F 2004 *PhD Thesis* University of Milano
[20] Clément-Cottuz J, Amokrane S and Regnaut C 1999 *Phys. Rev.* E **61** 1692
[21] Meroni A, Parola A and Reatto L 1990 *Phys. Rev.* A **42** 6104
[22] Tau M, Parola A, Pini D and Reatto L 1995 *Phys. Rev.* E **52** 2644
[23] Verlet L and Weis J J 1972 *Phys. Rev.* A **5** 939
Henderson D and Grundke E W 1975 *J. Chem. Phys.* **63** 601
[24] Caccamo C, Pellicane G, Costa D, Pini D and Stell G 1999 *Phys. Rev.* E **60** 5533
[25] Louis A A 2002 *J. Phys.: Condens. Matter* **14** 9187
[26] Barker J A and Henderson D 1967 *J. Chem. Phys.* **47** 2856
[27] Weis J J 1974 *Mol. Phys.* **28** 187
Hecht C E and Lind J 1976 *J. Chem. Phys.* **64** 641
Kincaid J M, Stell G and Goldmark E 1976 *J. Chem. Phys.* **65** 2172
[28] Gast A P, Hall C K and Russel W B 1983 *J. Colloid Interface Sci.* **96** 251
[29] Hagen M H J and Frenkel D 1994 *J. Chem. Phys.* **101** 4093
[30] Hall K R 1972 *J. Chem. Phys.* **57** 2252
[31] Foffi G, McCullagh G D, Lawlor A, Zaccarelli E, Dawson K A, Sciortino F, Tartaglia P, Pini D and Stell G 2002 *Phys. Rev.* E **65** 031407
[32] Kincaid J M and Weis J J 1977 *Mol. Phys.* **34** 931
[33] Lado F, Foiles S M and Ashcroft N W 1983 *Phys. Rev.* A **28** 2374
[34] Caccamo C 1996 *Phys. Rep.* **274** 1
[35] Lo Verso F, Tau M and Reatto L 2003 *J. Phys.: Condens. Matter* **15** 1505
[36] Hansen J P and McDonald I R 1986 *Theory of Simple Liquids* (London: Academic)
[37] Lado F, Foiles S M and Ashcroft N W 1983 *Phys. Rev.* A **28** 2374
[38] Barker J A and Henderson D 1967 *J. Chem. Phys.* **47** 4714
[39] Götzelmann B, Evans R and Dietrich S 1998 *Phys. Rev.* E **57** 6785
[40] Barboy B and Gelbart W M 1979 *J. Chem. Phys.* **71** 3053
[41] Ballone P, Pastore G, Galli G and Gazzillo D 1986 *Mol. Phys.* **59** 275
[42] Parola A, Pini D and Reatto L 1993 *Phys. Rev.* E **48** 3321
[43] Pusey P N 1948 *Colloidal Suspension* ed J P Hansen, D Levesque and J Zinn-Justin (Amsterdam: Elsevier)
[44] Asakura S and Oosawa F 1954 *J. Chem. Phys.* **22** 1255
Asakura S and Oosawa F 1958 *J. Polym. Sci.* **33** 183
[45] Vrij A 1976 *Pure Appl. Chem.* **48** 471
[46] Ilett S M, Orrock A, Poon W C K and Pusey P N 1995 *Phys. Rev.* E **51** 1344
[47] Brader J M, Evans R and Schmidt M 2003 *Mol. Phys.* **101** 3349
[48] Lekkerkerker H N W, Poon W C K, Pusey P N, Stroobans A and Warren P B 1992 *Europhys. Lett.* **20** 559
[49] Leal Calderon F, Bibette J and Biais J 1993 *Europhys. Lett.* **23** 653
[50] Meijer E J and Frenkel D 1994 *J. Chem. Phys.* **100** 6873
[51] Noro M G and Frenkel D 2000 *J. Chem. Phys.* **113** 2941
[52] Louis A A 2002 *Preprint* cond-mat/0212073
[53] Fisher M E 1968 *Phys. Rev.* **176** 257
Saam W F 1970 *Phys. Rev.* A **2** 1461
[54] See, for instance, Fisher M E 1982 *Critical Phenomena* (*Lecture Notes in Physics* vol 186) ed F J W Hahne (Berlin: Springer)
[55] ten Wolde P R and Frenkel D 1997 *Science* **277** 1975